Received: 23 June 2018 | Accepted: 6 November 2018

DOI: 10.1002/jcp.27791

ORIGINAL RESEARCH ARTICLE

WILEY Journal of Cellular Physiology

Ranolazine prevents pressure overload-induced cardiac hypertrophy and heart failure by restoring aberrant Na^+ and Ca^{2+} handling

Jiali Nie[1,2] | Quanlu Duan[1,2] | Mengying He[1,2] | Xianqing Li[1,2] | Bei Wang[1,2] | Chi Zhou[1,2] | Lujin Wu[1,2] | Zheng Wen[1,2] | Chen Chen[1,2] | Dao Wu Wang[4] | Katherina M. Alsina[3] | Xander H.T. Wehrens[3] | Dao Wen Wang[1,2] | Li Ni[1,2,3]

[1]Division of Cardiology, Department of Internal Medicine, Tongji Hospital, Tongji Medical College, Huazhong University of Science and Technology, Wuhan, China

[2]Hubei Key Laboratory of Genetics and Molecular Mechanisms of Cardiological Disorders, Wuhan, China

[3]Department of Molecular Physiology & Biophysics and Department of Medicine, Cardiovascular Research Institute, Cardiology Baylor College of Medicine, Houston, Texas

[4]Department of Cardiology, The First Affiliated Hospital, Nanjing Medical University, Nanjing, China

Correspondence
Li Ni, MD, PhD, Division of Cardiology, Department of Internal Medicine, Tongji Hospital, Tongji Medical College, Huazhong University of Science and Technology, 430030 Wuhan, China.
Email: nili@tjh.tjmu.edu.cn

Funding information
National Natural Science Foundation of China, Grant/Award Numbers: 81470519, 81630010, 31400998, 91439203, 31771264; National Institutes of Health, Grant/Award Numbers: R01-HL089598, R01-HL091947, R01-HL117641; American Heart Association, Grant/Award Number: 13EIA14560061

Abstract

Background: Cardiac hypertrophy and heart failure are characterized by increased late sodium current and abnormal Ca^{2+} handling. Ranolazine, a selective inhibitor of the late sodium current, can reduce sodium accumulation and Ca^{2+} overload. In this study, we investigated the effects of ranolazine on pressure overload-induced cardiac hypertrophy and heart failure in mice.

Methods and Results: Inhibition of late sodium current with the selective inhibitor ranolazine suppressed cardiac hypertrophy and fibrosis and improved heart function assessed by echocardiography, hemodynamics, and histological analysis in mice exposed to chronic pressure overload induced by transverse aortic constriction (TAC). Ca^{2+} imaging of ventricular myocytes from TAC mice revealed both abnormal SR Ca^{2+} release and increased SR Ca^{2+} leak. Ranolazine restored aberrant SR Ca^{2+} handling induced by pressure overload. Ranolazine also suppressed Na^+ overload induced in the failing heart, and restored Na^+-induced Ca^{2+} overload in an sodium-calcium exchanger (NCX)-dependent manner. Ranolazine suppressed the Ca^{2+}-dependent calmodulin (CaM)/CaMKII/myocyte enhancer factor-2 (MEF2) and CaM/CaMKII/calcineurin/nuclear factor of activated T-cells (NFAT) hypertrophy signaling pathways triggered by pressure overload. Pressure overload also prolonged endoplasmic reticulum (ER) stress leading to ER-initiated apoptosis, while inhibition of late sodium current or NCX relieved ER stress and ER-initiated cardiomyocyte apoptosis.

Conclusions: Our study demonstrates that inhibition of late sodium current with ranolazine improves pressure overload-induced cardiac hypertrophy and systolic and diastolic function by restoring Na^+ and Ca^{2+} handling, inhibiting the downstream hypertrophic pathways and ER stress. Inhibition of late sodium current may provide a new treatment strategy for cardiac hypertrophy and heart failure.

KEYWORDS
Heart failure, hypertrophy, $I_{Na,L}$, Ca^{2+} transient, ranolazine

Abbreviations: ANP, Atrial natriuretic peptide; ATF4, Activating transcription factor 4; BNP, Brain natriuretic peptide; CaM, Calmodulin; CaMKII, Calcium/calmodulin-dependent protein kinase II; CHOP, CCAAT-enhancer-binding protein homologous protein; CNα, Calcineurin α subunit; EF, Ejection fraction; ER, Endoplasmic reticulum; GRP78, Glucose-regulated protein 78; HDAC, Histone deacetylase; HF, Heart failure; $I_{Na,L}$, Late sodium current; LTCC, L-type calcium channel; MEF2D, Myocyte enhancer factor 2D; NCX, Sodium calcium exchanger; NFAT, Nuclear factor of activated T cells; RyR_2, Type II ryanodine receptor; TAC, Transverse aortic constriction; UPR, Unfolded protein response.

1 | INTRODUCTION

The prevalence of heart failure (HF) has increased over the last decade (Lou, Janardhan, & Efimov, 2012). Although pharmacotherapies significantly improve survival, the prognosis of HF is still relatively poor (Kaye & Krum, 2007). Defective intracellular Ca^{2+} handling is central to the depressed contractility and diminished contractile reserve observed in HF (Wehrens & Marks, 2004). Elevated Ca^{2+} levels lead to increased Ca^{2+} binding with inactive calmodulin (CaM) to form active CaM, and hypertrophic cascades involving Ca^{2+}/CaM/CaMKII/myocyte enhancer factor-2 (MEF2) and CaM/CaMKII/calcineurin/nuclear factor of activated T-cells (NFAT) may be triggered (Zhang et al., 2007). In addition, excessive Ca^{2+} levels increase phosphorylation of type II ryanodine receptor (RyR2) and more Ca^{2+} leaks from the sarco/endoplasmic reticulum through RyR2, aggravating cytoplasmic Ca^{2+} overload (Fischer et al., 2013, 2015; Popescu, Galice, Mohler, & Despa, 2016). Furthermore, cytoplasmic Ca^{2+} overload and exhausted Ca^{2+} stores disturb the environment for protein folding and lead to unfolded protein response (UPR) and endoplasmic reticulum (ER) stress (Hayashi & Su, 2007). ER-initiated apoptosis contributes to cardiac myocyte apoptosis in failing hearts (Ni et al., 2011).

Thus, an early and sustained reduction in intracellular Ca^{2+} may slow the progression of HF. However, long-term reduction of intracellular Ca^{2+} overload with the L-type Ca^{2+} channel blockers have the potential for adverse effects including bradycardia, hypotension, and exercise intolerance (St-Onge et al., 2014). An alternative therapeutic option to reduce intracellular Ca^{2+} overload in the failing heart is pharmacological inhibition of the late Na^+ current ($I_{Na,L}$) using a clinically available, selective inhibitor, ranolazine. $I_{Na,L}$ constitutes a very small portion of the inward sodium current under physiological conditions (Glynn et al., 2015). However, during pathological situations such as pressure overload, $I_{Na,L}$ increases and generates a considerable amount of sodium inward current, causing intracellular Ca^{2+} accumulation (Armoundas, Hobai, Tomaselli, Winslow, & O'Rourke, 2003; Maltsev, Silverman, Sabbah, & Undrovinas, 2007; Onal, Gratz, & Hund, 2017; Toischer et al., 2013). Ranolazine is an anti-ischemic and antianginal agent that inhibits the late Na^+ current, thereby normalizing intracellular Na^+ and potentiating Ca^{2+} extrusion from the cytosol via the Na^+–Ca^{2+} exchanger (NCX), ultimately relieving Ca^{2+} overload (Gaborit et al., 2005).

Ranolazine has shown beneficial effects in improving diastolic function in a HF dog model and in patients with coronary artery disease (Figueredo et al., 2011; Rastogi et al., 2008). However, the mechanism of long-term $I_{Na,L}$ inhibition with ranolazine in HF has not been fully explored. Toward this goal, transverse aortic constriction (TAC) induced pressure overload mice were implanted with the subcutaneous osmotic minipumps containing ranolazine or vehicle. Our data demonstrate that ranolazine prevents pressure overload-induced cardiac hypertrophy and HF and restores aberrant intracellular Na^+ and Ca^{2+} handling. In addition, these data revealed that ranolazine inhibits Ca^{2+}/CaMKII-dependent signaling pathways and ER stress induced in failing hearts. Our study prompts ranolazine as a potential candidate for treating pressure overload-induced cardiac hypertrophy and HF.

2 | MATERIALS AND METHODS

2.1 | Materials

Ranolazine (R6152), tetracaine (T7508), Claycomb medium (51800C), and Liberase™ (5401151001) were purchased from Sigma-Aldrich (St. Louis, MO). Veratridine (sc-201075) and sodium-binding benzofuran isophthalate-AM (SBFI-AM; sc-215841A), NCX (sc-32881), and glyceraldehyde 3-phosphate dehydrogenase (GAPDH; sc-293335) antibodies were from Santa Cruz Biotechnology (Dallas, TX). Caffeine (14118) was from Cayman Chemical (Ann Arbor, MI). SEA0400 (A3811) was from Apex Bio Technology (Houston, TX). Isoproterenol hydrochloride (I0260) was from Tokyo Chemical Industry (Tokyo, Japan). Bay K8644 (B112) was purchased from Selleckchem (Houston, TX). Fluo 4-AM (F14201) and CaMKII-t286 (PA5–35501) antibody were from Thermo Fisher Scientific (Waltham, MA). Actin tracker green (C1033) was from Beyotime Technology (Shanghai, China). Osmotic minipump (1004) was from Alzet (Cupertino, CA). Antibodies for glucose-regulated protein 78 (GRP78; 11587-1-AP), MEF2D (14353-1-AP), CCAAT-enhancer-binding protein homologous protein (CHOP; 15204-1-AP), atrial natriuretic peptide (ANP; 27426-1-AP), and CaMKII total (15443-1-AP) were purchased from Proteintech (Wuhan, China). Antibodies for brain natriuretic peptide (BNP; A2179), NFATc3 (A6666), and Histone H3 (Hist3.1, A10880) were from ABclonal Technology (Wuhan, China). Antibody for CNα (M03026) was from Boster Biological Technology (Wuhan, China).

2.2 | Animal models

All animal experimental protocols complied with the "Guide for the Care and Use of Laboratory Animals" published by the United States National Institutes of Health. The study was approved by the Institutional Animal Research Committee of Tongji Medical College. All animals were housed at the animal care facility of Tongji Medical College at 25°C with 12–12 hr light–dark cycles and allowed free access to normal mouse chow and water throughout the study period. Eight-week-old male C57BL/6J mice were randomly divided into different groups. Mice were anesthetized by a combination of ketamine (80 mg/kg) and xylazine (10 mg/kg) by intraperitoneal injection. The detailed protocol of TAC was as previously described and the needle size for constriction is 27G (deAlmeida, van Oort, & Wehrens, 2010). Ranolazine dissolved in saline was given by subcutaneous mini-pumps (40 $mg \cdot kg^{-1} \cdot d^{-1}$). The dosage was chosen according to the CARISA trial (Chaitman, 2004). In vitro study, 10 μmol/L ranolazine was used, because it is within the range of therapeutic plasma levels and inhibitory concentrations of 50% for inhibition of $I_{Na,L}$ (6–15 μmol/l; Toischer et al., 2013).

2.3 | Evaluation of cardiac function

An ultrasound machine with high resolution and equipped with a 30 MHz scan head was used to detect mice ventricular dimensions (Vevo1100; VisualSonics, Toronto, Canada). Echocardiography was performed on anesthetized mice as described previously (Toischer et al., 2013).

2.4 | In vivo hemodynamics

Mice were anaesthetized. A pressure–volume catheter (Millar 1.4 Fr, SPR 835, Millar Instruments, Inc., Houston, TX) was inserted into the left ventricle through the carotid artery for measurement of intraventricular pressure and volume as described previously (Cingolani, Yang, Cavasin, & Carretero, 2003).

2.5 | Histological analysis

Myocardial tissue was fixed with 4% paraformaldehyde at room temperature and embedded in paraffin. Heart sections were performed with wheat germ agglutinin, TdT-mediated dUTP nick-end labeling, Masson, Sirius red, hematoxylin/eosin following the instructions of manufacturers.

2.6 | Preparation of isolated cardiac myocytes

The mouse was anesthetized with a mixture of pentobarbital and heparin intraperitoneally. Mouse chest cavity was exposed using scissors and the heart was immediately removed and immersed into ice-cold Tyrode's buffer containing NaCl 125 mmol/L, KCl 5 mmol/L, hydroxyethyl piperazineethanesulfonic acid (HEPES) 15 mmol/L, $MgCl_2$ 1.2 mmol/L, and glucose 10 mmol/L, pH 7.35–7.38 (at 25°C), saturated oxygen. The aorta was then quickly mounted on the cannula. The heart was perfused with Tyrode buffer containing NaCl 125 mmol/L, KCl 5 mmol/L, HEPES 15 mmol/L, $MgCl_2$ 1.2 mmol/L, taurine 6 mmol/L, BDM 7.5 mmol/L, and glucose 10 mmol/L, pH 7.35–7.38 (at 25°C) for 5 min at 37°C. The perfusion buffer was then switched to enzymatic buffer (Tyrode buffer supplemented with 1 mg/40 ml liberase). Constant perfusion pressure of 120 cm H_2O was applied. When the drop rate accelerated suddenly, the perfusion was stopped. The atrial part was discarded while the ventricle part was cut into small tissue pieces and was pipetted gently. The digestion was stopped using Dulbecco's modified Eagle's medium (DMEM) containing 10% fetal bovine serum (FBS) when abundant isolate rod-like cardiac myocytes were visible by microscopy.

2.7 | Calcium imaging studies

Isolated ventricular myocytes were loaded with 5 μM Fluo 4-AM in Tyrode's buffer containing (in mM): 140 NaCl, four KCl, one $MgCl_2$, five HEPES, 10 glucose, 1.8 $CaCl_2$ (pH 7.4, 37°C) in 37°C for 30 min. Excess dye was washed away with Tyrode's buffer for 15 min. Myocytes were field stimulated at 0.5 Hz and the Metamorph imaging system from Universal Imaging Corporation (West, Chester, PA) was used to detect fluorescence at 488 nm excitation. The background was subtracted. The Ca^{2+} transient was denoted as F/F_0, where F_0 is the baseline fluorescence as previously described (de Almeida et al., 2013).

Myocytes were paced in Tyrode's buffer containing 1.8 mM Ca^{2+}. The perfusion was then switched to Tyrode's buffer containing 1 mM tetracaine and 0 mM Ca^{2+} to block SR leak through RyR2 for 5 min. Then the perfusion was switched to normal Tyrode's buffer plus 10 mM caffeine to empty sarcoplasmic/endoplasmic Ca^{2+} storage. The percentage of SR leak was then calculated as previously described (Chelu et al., 2009).

2.8 | Determination of intracellular Na^+ concentration

Isolated ventricular myocytes were loaded with 5 μM SBFI-AM in Tyrode's buffer in 37°C for 30 min. Myocytes were washed with Tyrode's buffer for 15 min and were excited at 340 and 380 nm, respectively. The background fluorescence was determined as the cell before loading. The ratio F_{340}/F_{380} was calculated from the background-subtracted emission intensities to represent intracellular Na^+ as previously described (Wagner et al., 2006).

2.9 | Cell culture

HL-1 cells were cultured using Claycomb method. Claycomb medium was purchased from Sigma-Aldrich and was supplemented with 100 μM norepinephrine, 10% FBS, and 4 mM L-glutamine. HL-1 cells were pretreated with 20 μM isoproterenol hydrochloride (Iso), 1 μM Bay K8644 (Bay), 30 μM veratridine (Ver) for 24 hr, respectively. Ranolazine (Ran; 10 μM), SEA0400 (SEA; 1 μM), nifedipine (Nif; 1 μM) were incubated for 24 hr, followed by harvest.

2.10 | Flow cytometry

Cardiomyocyte apoptosis was evaluated using Annexin-V/propidium iodide (PI) apoptotic assay according to the manufacturer's instructions (KGA108; Jiangsu KeyGEN BioTECH Corp., Ltd, Nanjing, China).

2.11 | Extraction of cytoplasmic and nuclear proteins

Extraction of cytoplasmic and nuclear proteins from myocardium was performed using hypotonic cytoplasmic extraction (CE) buffer and high salt nuclear extraction (NE) buffer. Briefly, homogenize 50 mg tissue using a TissueLyser LT (Qiagen N.V., Venlo, The Netherlands), add 500 μl CE buffer (HEPES 10 mM, NaF 20 mM, Na_3VO_4 1 mM, KCl 60 mM, EDTA 1 mM, EGTA 1 mM, and DTT 2 mM, with protease inhibitors and phosphatase inhibitors), incubate the in EP tube on ice for 10 min, add ice-cold 50 μl 5% NP-40, vortex and incubate on ice for 1 min, centrifuge 1,500*g* for 5 min, transfer supernatant to a new

EP tube, centrifuge 16,000*g* for 20 min, the supernatant is the cytoplasmic fraction. Add 1 ml of CE buffer (without protease and phosphatase inhibitors) to pellet above, resuspend and wash the pellet three times by centrifuging 1,500*g* for 5 min, remove supernatant, add 250 μl NE buffer (HEPES 10 mM, NaF 20 mM, Na_3VO_4 1 mM, KCl 60 mM, EDTA 1 mM, EGTA 1 mM, DTT 2 mM, NaCl 420 mM, and glycerol 0.2 mM, with protease inhibitors and phosphatase inhibitors), resuspend and incubate on ice for 10 min, sonicate three times for 1 s each on ice, centrifuge 16,000*g* for 20 min, the supernatant is the nuclear fraction.

For nuclear extraction of cultured cells, cells were scraped in cold phosphate-buffered saline, spun down (12,000*g*, 30 s), resuspended in 400 μl CE buffer with 25 μl of 10% NP-40 and then spun down. Nuclei in the pellet were resuspended in NE buffer, and protein concentration was determined.

2.12 | Western blot analysis

Cells and cardiac tissue were extracted using Protein or IP lysate (Beyotime Technology, Shanghai, China) containing 1:100 protease inhibitor and 1:100 phosphatase inhibitor, and the protein concentration was calculated by Bicinchoninic Acid Assay Kit (Boster, Wuhan, China). A total of 10% and 6–12% gradient gels were used. Antibodies were diluted by 1:1,000. Gel Pro analysis software was used for quantification.

2.13 | RNA extraction and quantitative reverse-transcription polymerase chain reaction (qRT-PCR)

Total RNA was extracted using TRIzol (Invitrogen, Carlsbad, CA). Reverse-transcription was performed using MultiScribe system (ABI, Waltham, MA) for complementary DNA (cDNA). 7900HT Fast Real-Time PCR System was used for real-time PCR. The messenger RNA (mRNA) level was compared according to the comparative threshold cycle $2^{-\Delta\Delta C_t}$ method. Primers were designed using Primer 5.0 (PREMIER Biosoft, Palo Alto, CA) and verified using MFE 2.0 system (Qu et al., 2012). The primer sequences are listed in Supporting Information Table 3.

2.14 | Statistical analysis

Data were expressed as mean ± standard error of the mean. Comparisons among groups were performed by Student's *t*-test or one-way analysis of variance with post hoc analysis using the Student-Newman–Keuls method. Significance was accepted at $p < 0.05$.

3 | RESULTS

3.1 | Ranolazine blunts cardiac hypertrophy, fibrosis, and improved impaired cardiac function induced by pressure overload

We subjected male C57BL/6J mice to constriction of the transverse aorta (TAC) or to sham surgery for 4–9 weeks. The mice were concurrently subcutaneously implanted with osmotic mini-pumps of ranolazine (40 $mg \cdot kg^{-1} \cdot d^{-1}$) or vehicle saline. As shown in Figure 1, TAC-induced left ventricular and cellular hypertrophy. Both the hypertrophy and the chamber remodeling were inhibited by ranolazine in TAC mice (Figure 1a–g), whereas ranolazine had no impact on sham-operated groups. TAC also induced myocardial fibrosis which was suppressed by ranolazine (Figure 1l–n).

Detailed examination of heart function was carried out by invasive pressure–volume analysis. As shown in Figure 1i,j, cardiac function of TAC mice was decreased in comparison with the sham group as evidenced by the markedly reduced dP/dtmax and dP/dtmin, and administration with ranolazine resulted in a restoration in cardiac function. Serial echocardiography showed reduced fractional shortening (FS) and ejection fraction (EF) in mice 9 weeks after TAC surgery, and ranolazine preserved both FS and EF in TAC mice (Figure 1d,g,h,k and Supporting Information Table 1), indicating ranolazine prevented pressure overload-induced HF.

3.2 | Ranolazine restores aberrant SR Ca^{2+} handling induced by pressure overload

We determined intracellular Ca^{2+} state *in situ*. Ventricular myocytes were isolated and paced at 0.5 Hz to obtain steady-state Ca^{2+} handling. There was an increase in steady-state Ca^{2+} transient amplitude (CaT) in myocytes isolated from mice 4 weeks after TAC, and a reduction in CaT was observed in myocytes from mice 9 weeks after TAC operation (Figure 2a,b). Rapid application of tetracaine (TTc) and caffeine revealed decreased SR Ca^{2+} content at 9 W (Figure 2c), and increased SR Ca^{2+} leakage was observed (Figure 2a,d) in myocytes from mice both at 4 W and 9 W after TAC. Administration of ranolazine restored the altered Ca^{2+} kinetics induced by pressure overload (Figure 2 and Supporting Information Figure S1).

To investigate the effect of ranolazine in vitro, cardiomyocytes were isolated from control C57/BL mice, and treated with isoproterenol hydrochloride (Iso), a hypertrophic stimulus and L-type calcium channel (LTCC) activator Bay K8644 (Bay) which can induce intracellular Ca^{2+} overload. Ranolazine reduced the increasing CaT amplitude stimulated by Iso and Bay (Figure 2e,f). Overall, these findings indicate that ranolazine restores aberrant SR Ca^{2+} storage and Ca^{2+} release and relieves Ca^{2+} load induced by pressure overload.

3.3 | Ranolazine restores aberrant Ca^{2+} handling induced by Na^+ overload

Since ranolazine is an inhibitor of late sodium current, we tested the intracellular Na^+ level using SBFI-AM. As shown in Figure 3a, Na^+ level was increased in TAC mice both at 4 weeks and 9 weeks, and administration of ranolazine alleviated such Na^+ overload. In vitro study, we used a sodium channel agonist veratridine to induce intracellular Na^+ overload in isolated ventricular myocytes of control mice (Brill & Wasserstrom, 1986; Kent, Hoober, & Cooper, 1989), and ranolazine relieved intracellular Na^+ overload induced by veratridine (Figure 3b).

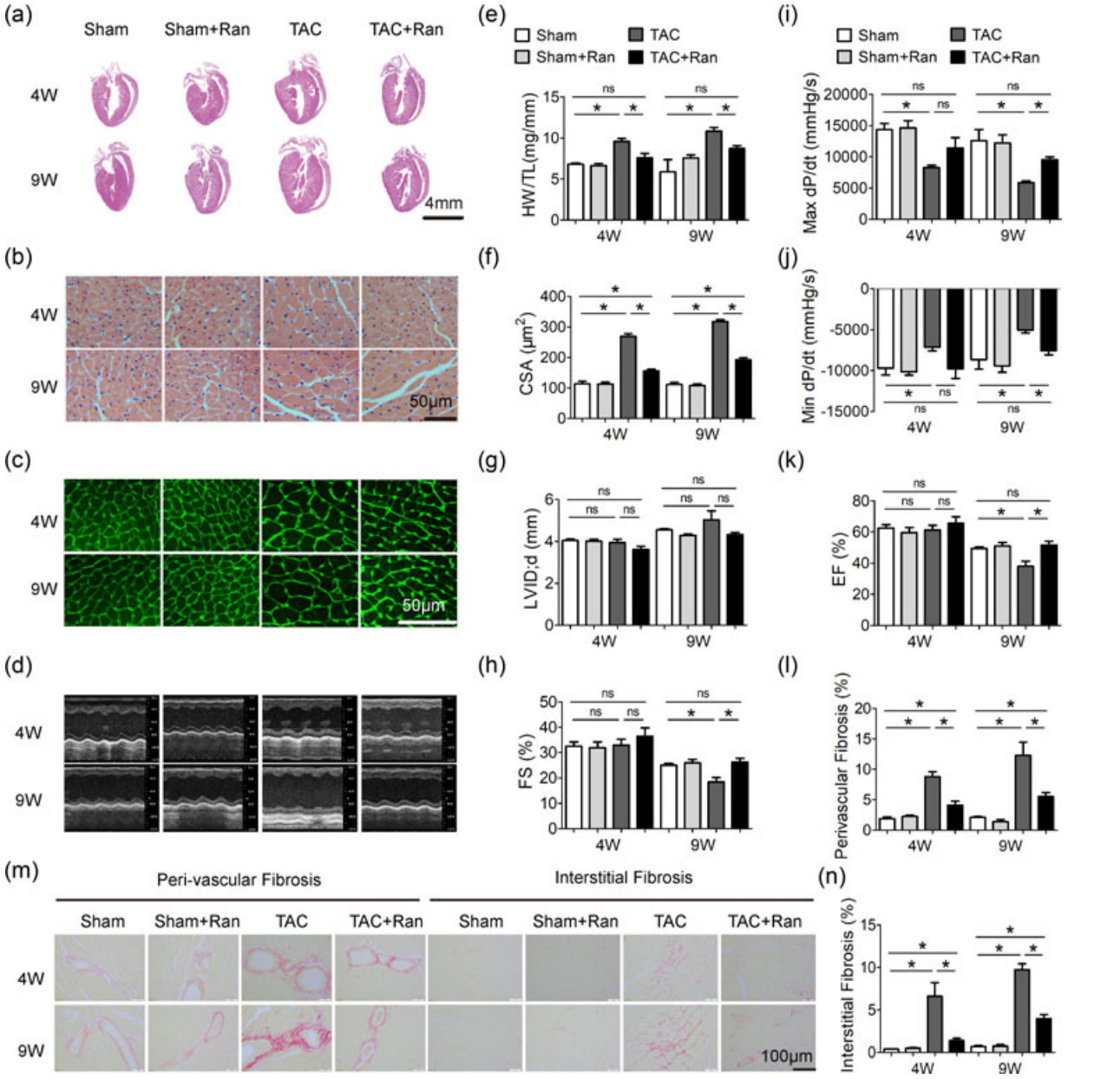

FIGURE 1 Ranolazine-blunts pressure overload-induced cardiac hypertrophy and heart failure. (a) Examples of HE staining of heart sections. Examples of HE staining (b) and Wheat germ agglutinin staining (c) of heart cross-sections. (d) M-mode echocardiogram. (e) Statistics of HW/TL. (f) Statistics of CSA. (g) Statistics of LVID (d) by echocardiography. (h) Statistics of FS by echocardiography. Quantification of max d*P*/d*t*, peak rate of pressure increase (i), and min d*P*/d*t*, peak rate of pressure decline (j), measured by aortic catheterization. (k) Statistics of EF by echocardiography. Sirius red stained myocardium section (m) and quantification (l and n) of cardiac fibrosis. Mice number was 5–14 per group. One-way ANOVA was performed for groups with the same intervention time; e.g., in (e), HW/TL values of Sham, Sham + Ran, TAC, and TAC + Ran at 4 weeks were compared using one-way ANOVA, while HW/TL values of Sham, Sham + Ran, TAC, and TAC + Ran at 9 weeks were compared using another one-way ANOVA independently. The same went for the rest of statistics. All data were shown as mean ± standard error of the mean ($n \geq 5$; $^*p < 0.05$). ANOVA: analysis of variance; CSA: cross sectional area; EF: ejection fraction; FS: fractional shortening; HW/TL: heart weight/tibia length; LVID: left ventricular internal diameter at diastole; Ran: ranolazine dyhydrocloride; TAC: transverse aortic constriction surgery; 4 W, 9 W: 4 weeks or 9 weeks after TAC operation [Color figure can be viewed at wileyonlinelibrary.com]

Since NCX plays the bridging role between Na^+ and Ca^{2+}, SEA0400 (SEA), an inhibitor of NCX activity, was utilized. We investigated the relationship between Na^+ overload and Ca^{2+} signaling in mouse ventricular myocytes. As shown in Figure 3c-f, veratridine increased Ca^{2+} transient amplitude, impaired SR Ca^{2+} content and increased SR Ca^{2+} leak. Both ranolazine and NCX inhibitor were effective to normalize aberrant Ca^{2+} handling. In addition, ranolazine-reduced overexpression of NCX induced in TAC mice, Iso treated HL-1 cells and veratridine-treated HL-1 cells (Figure 3g–i).

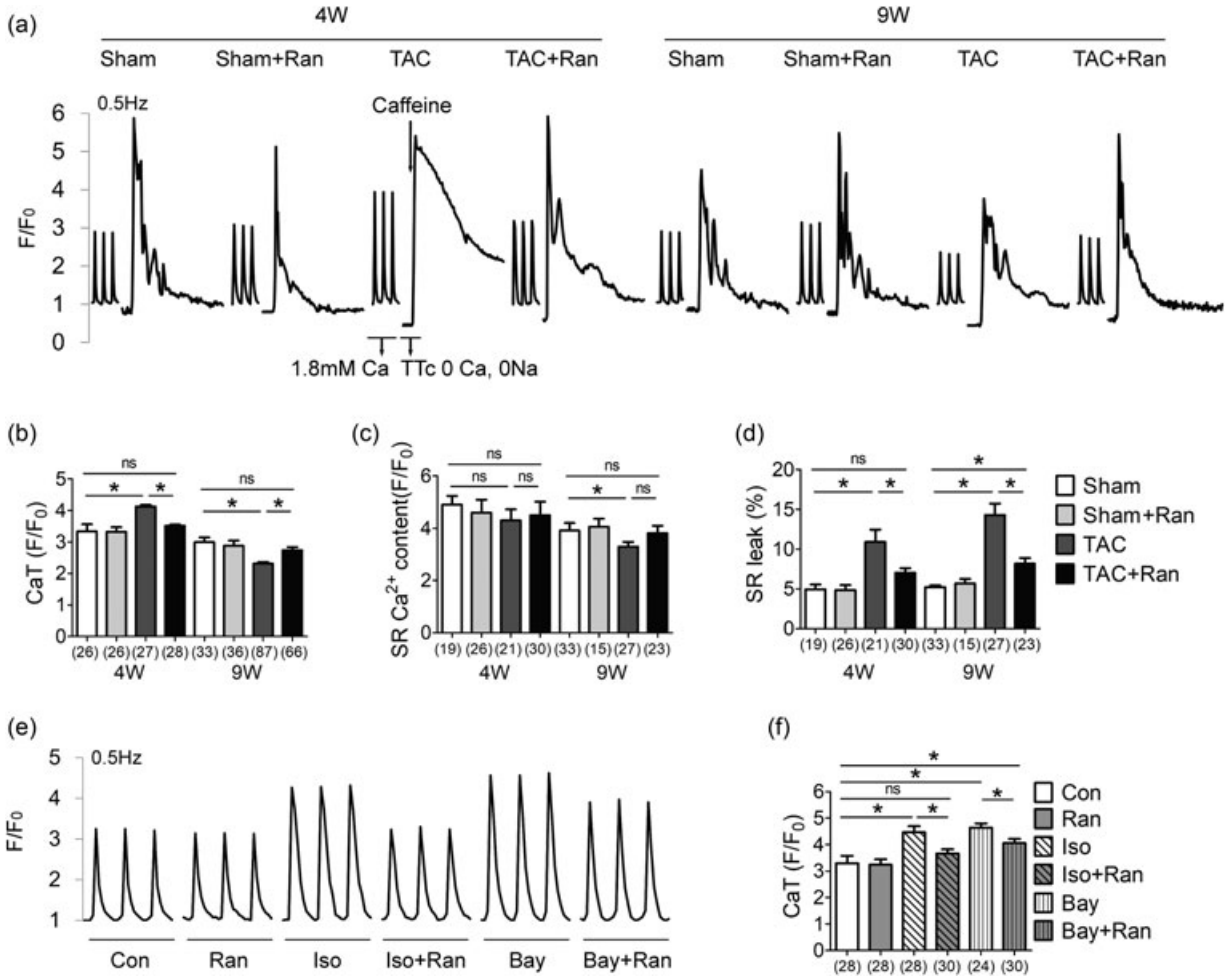

FIGURE 2 Ranolazine restores aberrant intracellular Ca^{2+} induced by pressure overload. (a) Representative Ca^{2+} recordings obtained in ventricular myocytes stimulated at 0.5 Hz. Ca^{2+} transient was recorded with Tyrode's perfusion containing 1.8 mM Ca^{2+}. SR leak was measured by switching the perfusion to 1 mM TTc buffer containing 0 Ca^{2+} and 0 Na^{+} to block SR leak, and caffeine was applied to empty SR Ca^{2+} storage. Quantification of CaT amplitude (b), SR Ca^{2+} content (c) and SR leak percentage (d). The Ca^{2+} transient recordings (e) and quantification (f) of the CaT amplitude in cardiomyocytes isolated from control C57/BL mice under different stimulus. Numbers indicate the number of cells for each condition (3–5 mice per group). Myocytes were concurrently treated with Bay/Iso and Ran 1 hr before the fluorescence detection. Ran, 10 μM; Iso, 20 μM; Bay, Bay K8644, LTCC activator, 1 μM. One-way ANOVA was performed for groups with the same intervention time; e.g., in (b), amplitude of CaT values of Sham, Sham + Ran, TAC and TAC + Ran at 4 weeks were compared using one-way ANOVA, while CaT values of Sham, Sham + Ran, TAC, and TAC + Ran at 9 weeks were compared using another one-way ANOVA independently. The same applied to (c,d). One-way ANOVA was performed for the analysis of (f). All data were shown as mean ± standard error of the mean (*$p < 0.05$). ANOVA: analysis of variance; Bay: Bay K8644; CaT: Ca^{2+} transient; Iso, isoproterenol hydrochloride; LTCC: L-type calcium channel; Ran: ranolazine dyhydrochloride; TAC: transverse aortic constriction surgery; TTc: tetracaine

Together, these data revealed ranolazine suppresses Na^{+} overload in cardiac hypertrophy, and prevents Na^{+} induced Ca^{2+} mishandling in an NCX-dependent manner.

3.4 | Ranolazine inhibits Ca^{2+}-dependent hypertrophic pathways

Elevated Ca^{2+} level leads to increased Ca^{2+} binding with inactive CaM to form active CaM, which may trigger the hypertrophic Ca^{2+}/CaM/CaMKII/MEF2 cascade. Since aberrant Ca^{2+} cycling was observed in TAC mice (Figure 2), we tested the activation state of the Ca^{2+}-dependent hypertrophic pathway. In hearts exposed to pressure overload, CaMKII was highly phosphorylated at the 286 threonine (Figure 4a). CaMKII-t286 can, in turn, phosphorylate histone deacetylase (HDAC) and release MEF2D from HDAC transcription suppression. MEF2D upregulated hypertrophic gene expression, as evidenced by ANP and BNP from protein (Figure 4b) and mRNA levels (Supporting Information Figure S2A). While in mice treated with ranolazine, this hypertrophic cascade was well inhibited.

Additionally, activation of the calcineurin/NFAT pathway was observed in TAC mice. NFAT is a group of transcription factors that modulate cell cycle, differentiation and apoptosis (Mognol, Carneiro, Robbs, Faget, & Viola, 2016). Under physiological situations, NFAT stays in the cytoplasm in a phosphorylated state. In response to Ca^{2+}

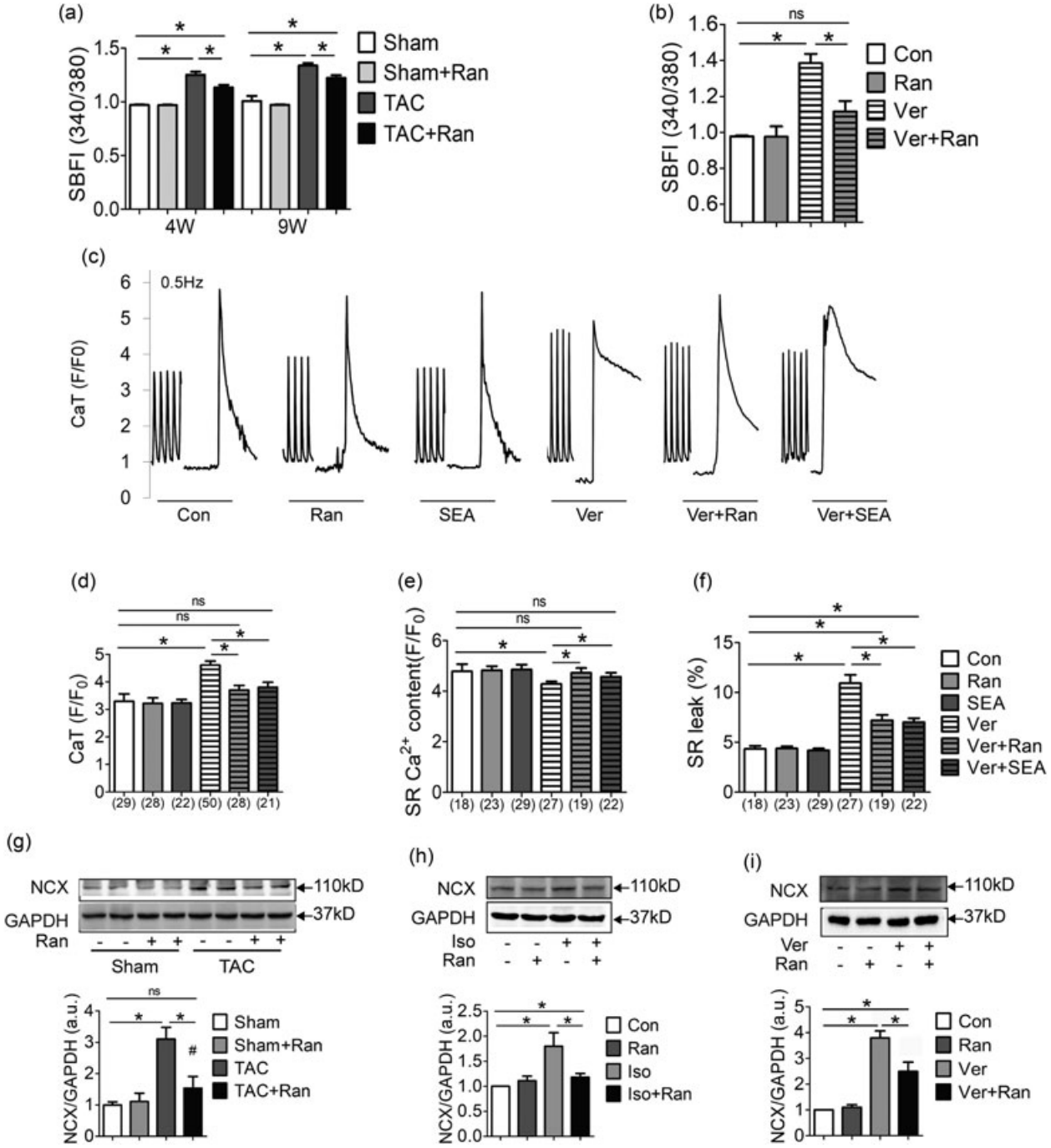

FIGURE 3 Ranolazine suppresses Na^+ induced Ca^{2+} overload via NCX in the failing heart. (a) Fluorescence ratio of SBFI-AM staining to mearure intracellular Na^+ (3–5 mice per group). (b) Intracellular Na^+ change in response to Ver and Ran treatment. Cardiomyocytes were isolated from control C57/BL mice (replicates $n \geq 5$ per group). Myocytes were concurrently treated with Ver and Ran 1 hr before the SBFI-AM fluorescence detection. Representative Ca^{2+} recordings (c) and quantification of CaT amplitude (d), SR Ca^{2+} content (e) and SR leak percentage (f) of contol C57/BL mouse cardiomyocytes in response to Ver, Ran, and SEA. Drugs were given concurrently to myocytes for 1 hr before Fluo 4-AM fluorescence detection. Numbers indicate the number of cells for each condition. (g) NCX expression in mice after 4 weeks. NCX expression in Iso treated HL-1 cells (h) and Ver treated HL-1 cells (i). HL-1 cells were treated with Iso, Ver, Ran, or SEA for 24 hr before protein extraction. Each western blot analysis was performed for 3–5 biological repeats. For (a) the 340/380 ratio of Sham, Sham + Ran, TAC, and TAC + Ran at 4 weeks were compared using one-way ANOVA, while 340/380 ratio of Sham, Sham + Ran, TAC and TAC + Ran at 9 weeks were compared using another one-way ANOVA independently. One-way ANOVA was applied for the statistic of (b,d-i). All data were shown as mean ± standard error of the mean (*$p < 0.05$). ANOVA: analysis of variance; Bay: Bay K8644; CaT: Ca^{2+} transient; Iso: isoproterenol hydrochloride; LTCC: L-type calcium channel; NCX: sodium calcium exchanger; Ran: ranolazine dyhydrochloride; SBFI-AM: sodium-binding benzofuran isophthalate-AM; SEA: SEA0400; TAC, transverse aortic constriction surgery; TTc: tetracaine; Ver: veratridine

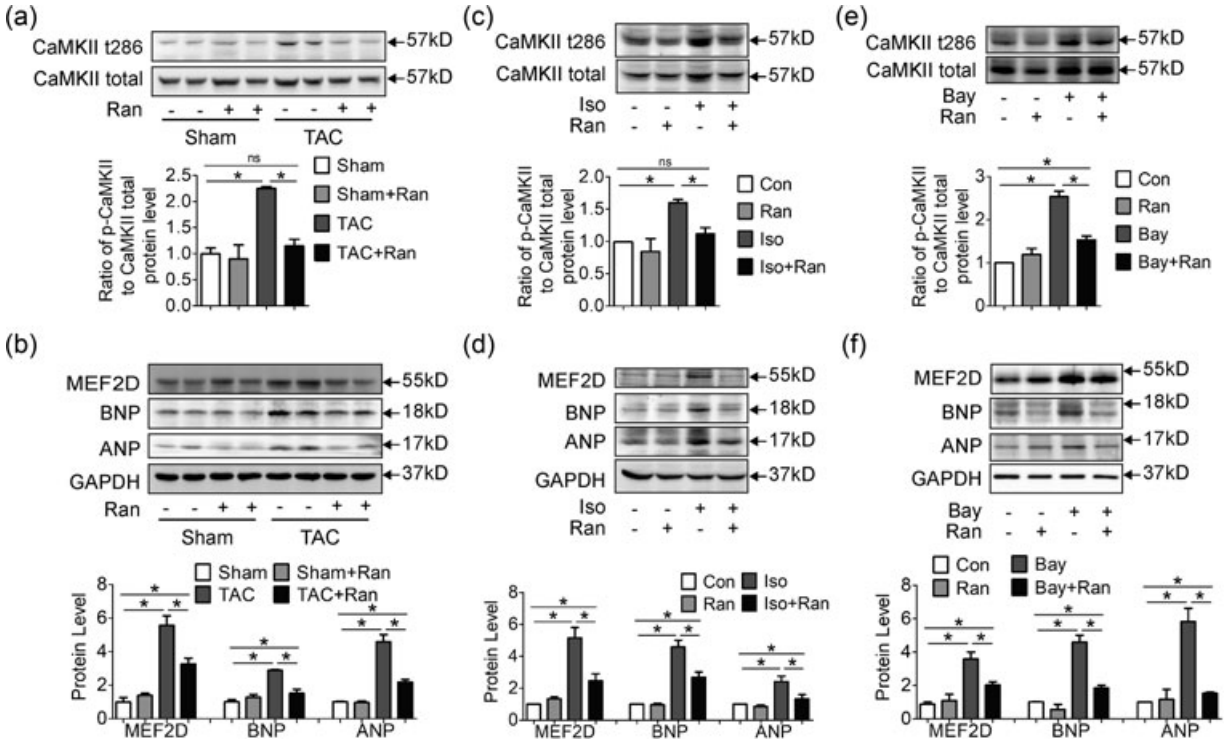

FIGURE 4 Ranolazine inhibits Ca^{2+}-dependent Ca^{2+}/CaM/CaMKII/MEF2D hypertrophic pathway. (a, b) Western blot analysis of myocardium lysate at 4 weeks. CaMKII was highly phosphorylated in TAC mice, and the downstream hypertrophic markers MEF2D, ANP, and BNP were upregulated, while in ranolazine treated TAC mice, this pathway was inhibited. Hypertrophic markers were also tested in mouse cardiomyocyte cell line HL-1 exposed to Iso (c, d) or Bay (e, f). Each western blot analysis was performed for 3–5 biological repeats. One-way analysis of variance was used for analysis. Data were shown as mean ± standard error of the mean (*$p < 0.05$). ANP: atrial natriuretic peptide; Bay: Bay K8644; BNP: brain natriuretic peptide; CaM: calmodulin; Iso: isoproterenol hydrochloride; MEF2: myocyte enhancer factor-2; TAC: transverse aortic constriction surgery

overload, calcineurin would be activated by p-CaMKII to dephosphorylate NFAT. Dephosphorylated NFAT then enters the nuclei and modulates its target genes. Among the four isoforms of NFAT, NFATc3 is well-documented in mediating the hypertrophic signaling pathway (Wilkins & Molkentin, 2004). In this study, upregulation of calcineurin catalytic α subunit, CNα was detected in whole cell lysate of mouse myocardium (Figure 5b,c), followed by increased nuclear localization of NFATc3 (Figure 5a,c). In mice treated with ranolazine, CNα expression, and NFATc3 nuclear localization were significantly reduced.

In vitro hypertrophic stimuli Iso was applied to HL-1 cells and similar results were achieved for both the CaMKII/MEF2 (Figure 4c,d; Supporting Information Figure S2B and S2C) and the calcineurin/NFAT pathways (Figure 5d–f); indicating hypertrophic pathways induced by Iso were ameliorated by ranolazine.

To verify the antihypertrophic effect of ranolazine is by restoring altered Ca^{2+} handling than other mechanisms, the Ca^{2+} activator Bay was applied. As shown in Figure 4e,f, Supporting Information Figure 3d and Figure 5g–i, Ca^{2+}/CaM/CaMKII/MEF2 and calcineurin/NFAT pathways were triggered by Ca^{2+} overload and inhibited by ranolazine. Together, these data indicated that ranolazine probably exerts its protection by inhibiting Ca^{2+}-dependent hypertrophic pathways.

3.5 | Inhibition of late sodium current inhibits TAC-induced ER stress

Ca^{2+} overload and exhausted Ca^{2+} storage leads to UPR and endoplasmic reticulum (ER) stress. Sustained ER stress activates ER chaperones and CHOP expression, leading to cardiac myocyte apoptosis in failing hearts (Okada et al., 2004). Consistent with our previous study, we found that both mRNA and protein levels of ER stress markers GRP78, activating transcription Factor 4 (ATF4), and CHOP were increased in TAC mice, while ranolazine suppressed ER stress induced by pressure overload (Figure 6a,b; Ni et al., 2011). Similar results were observed in Iso and Bay treated HL-1 cells (Figure 6c–f). Ranolazine-reduced ER stress markers GRP78, ATF4, and CHOP induced by Iso and Bay. These data indicated that ranolazine relieves ER stress triggered by cardiac hypertrophy and Ca^{2+} overload.

CHOP is an apoptotic regulator. As shown in Figure 6a,b and Supporting Information Figure S4A, sustained ER stress and CHOP increase cell apoptosis in hypertrophic and failing hearts. In vitro apoptotic assay was assessed by annexin-V flow cytometry and inhibition of late sodium current by ranolazine effectively attenuated cell apoptosis under stimulation of Ca^{2+} (Bay) and Na^{+} activator (Ver; Supporting Information Figure S4B and S4C).

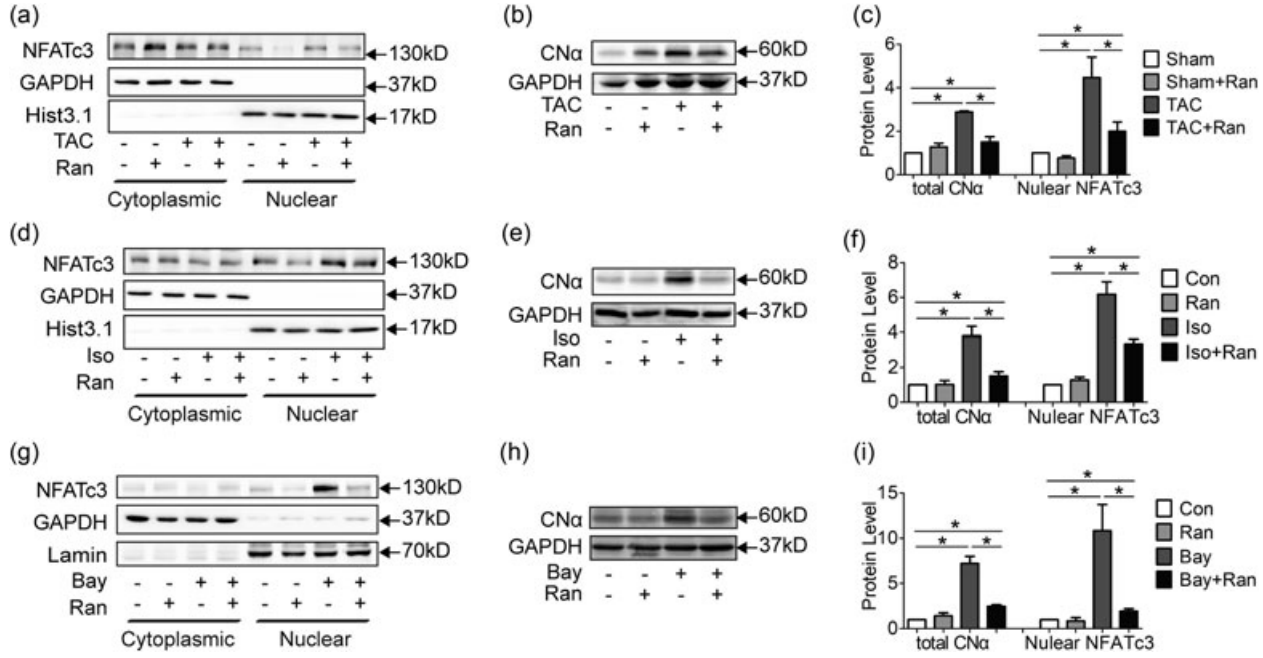

FIGURE 5 Ranolazine inhibits Ca^{2+}-dependent Ca^{2+}/calcineurin/NFAT hypertrophic pathway. (a) Cytoplasmic and nuclear proteins were extracted from mouse myocardium at 4 weeks for western blot analysis. GAPDH was taken as the cytoplasmic loading control. Histone H3 (Hist3.1) and Lamin B (Lamin) were taken as the nuclear loading control. Data showed that NFATc3 nuclear localization was increased in TAC mice and was significantly reduced by ranolazine. (b) Western blot analysis analysis of whole cell lysate revealed increased expression of calcineurin catalytic α subunit (CNα), which was reduced by ranolazine. (c) showed statistics of (a) and (b). CNα was also upregulated in Iso (e) and Bay (h) treated HL-1 cells, followed by increased nuclear localization of NFATc3 (d,g), and treatment with ranolazine significantly inhibited the calcineurin/NFAT pathway. Statistics were shown in (f) and (i). Each western blot analysis was performed for 3–5 biological repeats. One-way analysis of variance was used for analysis. Data were shown as mean ± standard error of the mean (*$p < 0.05$). GAPDH: glyceraldehyde 3-phosphate dehydrogenase; NFAT: nuclear factor of activated T-cells; TAC: transverse aortic constriction surgery

3.6 | Inhibition of NCX reduces Ca^{2+}-dependent hypertrophic pathway and ER stress

The sodium/calcium exchanger NCX is a key mediator of Na^+ and Ca^{2+} crosstalk. The physiological working mode of NCX is to carry Ca^{2+} out in exchange for Na^+ inward (Glynn et al., 2015). While in pathological situations like pressure overload, sustained $I_{Na,L}$ leads to elevated intracellular Na^+, which triggers the outward transfer mode of NCX to export Na^+ out and brings in more Ca^{2+} (Armoundas et al., 2003; Maltsev et al., 2007; Onal et al., 2017; Toischer et al., 2013). This also explains how the sodium channel agonist veratridine leads to increased CaT in Figure 3c. Since Na^+ activator leads to Ca^{2+} overload, we examined the state of Ca^{2+}-dependent hypertrophic pathway and ER stress in HL-1 cell line pretreated with veratridine.

As shown in Figure 7a,b, hypertrophic markers MEF2D, ANP and BNP and ER stress markers GRP78, ATF4, and CHOP were upregulated by sodium channel agonist veratridine, and reduced by inhibition of $I_{Na,L}$ with ranolazine. Also, inhibition of NCX activity with SEA0400 alleviated the hypertrophic pathway and ER stress triggered by veratridine (Figure 7c,d), highlighting the role of NCX in Na^+ induced Ca^{2+} overload. And flow cytometry suggested that inhibition of NCX effectively reduced veratridine induced cell apoptosis (Supporting Information Figure S3C). We further explored the role of SEA0400 in Iso pretreated HL-1 cells. As shown in Figure 7e,f, SEA0400 protected HL-1 cells from severe hypertrophy and ER stress. And depletion of NCX using NCX siRNA in HL-1 cells copied the observations in experiments with SEA0400 (Supporting Information Figure S5), implying the importance of NCX in cardiac hypertrophy and HF.

Above observations pointed to the importance of NCX in Na^+/Ca^{2+} crosstalk, and that inhibition of NCX activity alleviated Ca^{2+}-dependent hypertrophy and ER stress in cardiac hypertrophy and HF.

4 | DISCUSSION

In this study, we demonstrated the therapeutic effect of ranolazine in pressure overload-induced cardiac hypertrophy and HF, and the mechanisms underlying were through relieving Na^+-dependent Ca^{2+} overload and inhibiting ER stress and hypertrophic pathways as summarized in Figure 8.

Referring to the modeling characteristic of TAC surgery (Takimoto et al., 2005), 4 weeks after surgery was chosen as the time point of cardiac hypertrophy and HF with preserved ejection fraction (HFpEF), and 9 weeks after surgery as the time point of HF with reduced ejection fraction (HFrEF). Consistently, contractile function parameters such as EF, FS, and LVID; *d* were normal at 4 weeks and impaired at 9 weeks. As HF results from continuous remodeling rather than a sudden transformation. Genetic and

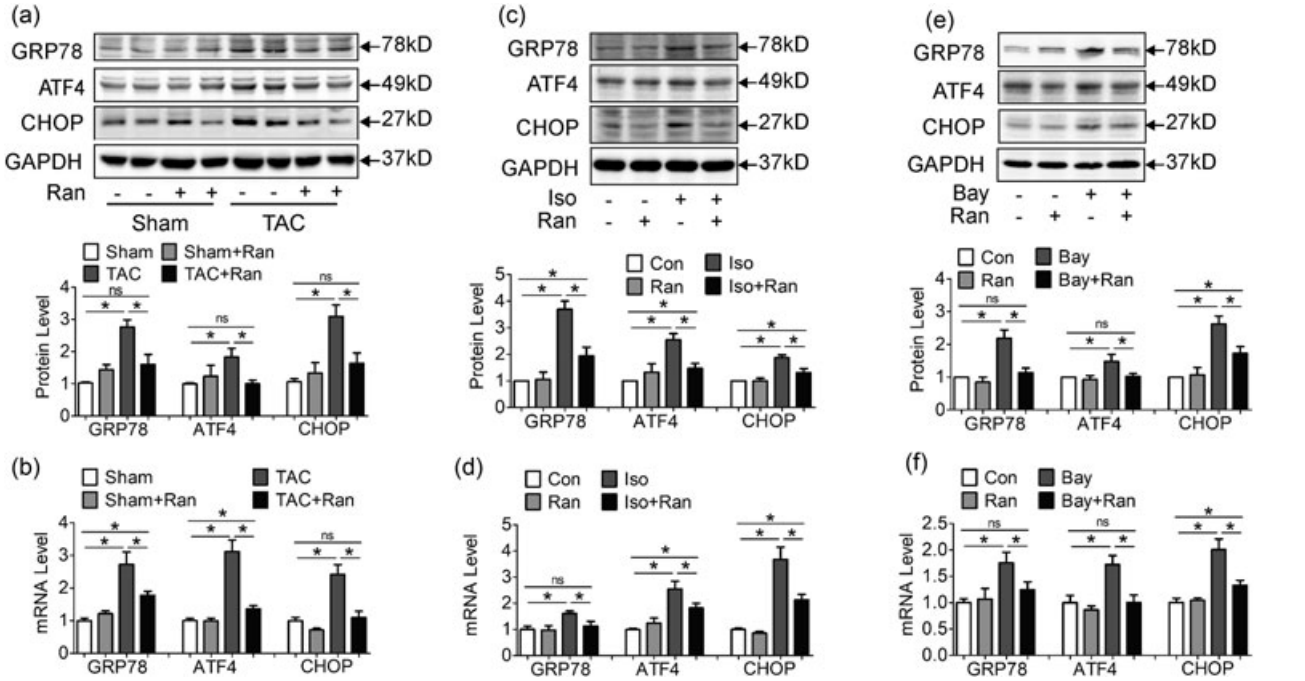

FIGURE 6 Ranolazine suppresses ER stress induced by pressure overload and Ca^{2+} overload. (a, b) Both protein level (a) and mRNA level (b) of ER stress markers GRP78, ATF4 and CHOP were increased in TAC mice at 4 weeks, while ranolazine suppressed ER stress induced by pressure overload. (c, d) ER stress markers increased in Iso pretreated HL-1 cells, while ranolazine inhibited ER stress at both protein and mRNA levels. (e, f) ER stress markers increased in LTCC activator Bay K8644 pretreated HL-1 cells, and ranolazine also reduced such ER stress at both protein and mRNA levels. Each western blot analysis was performed for 3–5 biological repeats. Real-time PCR was performed for three biological replicates, and three technical repeats for each replicate. One-way analysis of variance was used for analysis. Data were shown as mean ± standard error of the mean (*$p < 0.05$). ATF4: activating transcription factor 4; CHOP: CCAAT-enhancer-binding protein homologous protein; ER: endoplasmic reticulum; GRP78: glucose-regulated protein 78; LTCC: L-type calcium channel; mRNA, messenger RNA; PCR: polymerase chain reaction

microscopic alteration precedes the onset of impaired contractile function. Correspondingly, fibrotic deposition, cellular hypertrophy, Ca^{2+} dysregulation and gene changes were detected at 4 weeks, before the reduction of EF. One interesting finding in this study was that, while EF and FS by echocardiography were not altered, invasive pressure measurements showed a decline in function at 4 weeks in TAC mice. We attributed this discrepancy to impaired cardiac reserve of HFpEF (Henein, Morner, Lindmark, & Lindqvist, 2013). While cardiac function was compensated at resting state by echocardiography, the operation of invasive pressure measurements introduced a stress stimulus to the mouse cardiovascular system, exposing the impaired cardiac reserve at 4 weeks.

HF is the end stage of many cardiac diseases, and complex abnormalities are involved in the structural and functional remodeling. Ion dysregulation is a key aspect of cardiac remodeling. Studies have revealed aberrant dynamics of intracellular Na^+, K^+, and Ca^{2+}, accompanied by altered ion channel expression in HF. Late sodium current ($I_{Na,L}$) composes a lasting inward sodium current generated by delayed sodium channel inactivation. Increased $I_{Na,L}$ brings in more Na^+ into the cell and leads to intracellular Na^+ accumulation. Aberrant $I_{Na,L}$ is directly linked with increased susceptibility to arrhythmia and dysfunction in cardiac disease (Toischer et al., 2013). Recent studies demonstrated that sustained $I_{Na,L}$ was also causative to cardiac structural remodeling (Glynn et al., 2015). Data from patients and animal models all revealed enhanced $I_{Na,L}$ in hypertrophic cardiomyocytes (Coppini et al., 2013; Flenner et al., 2016; Toischer et al., 2013). Cellular Na^+ and Ca^{2+} homeostasis are tightly integrated, as cellular Na^+ overload stimulates the reverse mode of NCX to facilitate the influx of Ca^{2+} in exchange for efflux of Na^+. The net result is an elevated Ca^{2+} concentration. Ranolazine, a potent late $I_{Na,L}$ inhibitor, may normalize altered intracellular Ca^{2+} concentration due to the close relationship between Na^+ and Ca^{2+} handling by the Na^+/Ca^{2+} exchanger. Our study showed that ranolazine prevented cardiac hypertrophy and reduced myocardial fibrosis in a model of TAC-induced pressure overload by relieving Na^+-dependent Ca^{2+} overload.

SR Ca^{2+} leak is generated by increased opening probability (P_o) of RyR2. Parikh et al has proved that ranolazine-reduced P_o of RyR2 by stabilizing RyR2, though the mechanism remains unclear still (Parikh et al., 2012). Studies have shown that RyR2 is a phosphorylated substrate for kinase CaMKII, and hyper-phosphorylation of RyR2 at Ser2809 by CaMKII leads to increased P_o and SR leak, while activity of CaMKII is regulated by Ca^{2+} level (Fischer et al., 2013; Maier & Bers, 2007; Onal et al., 2017; Wehrens, Lehnart, Reiken, & Marks, 2004). In this study, we found that cardiac myocytes from TAC mice displayed decreased Ca^{2+} transient amplitudes due to reduced SR Ca^{2+} stores at the late stage of HF (9 weeks), while ranolazine treatment restored the altered SR Ca^{2+} stores induced by pressure

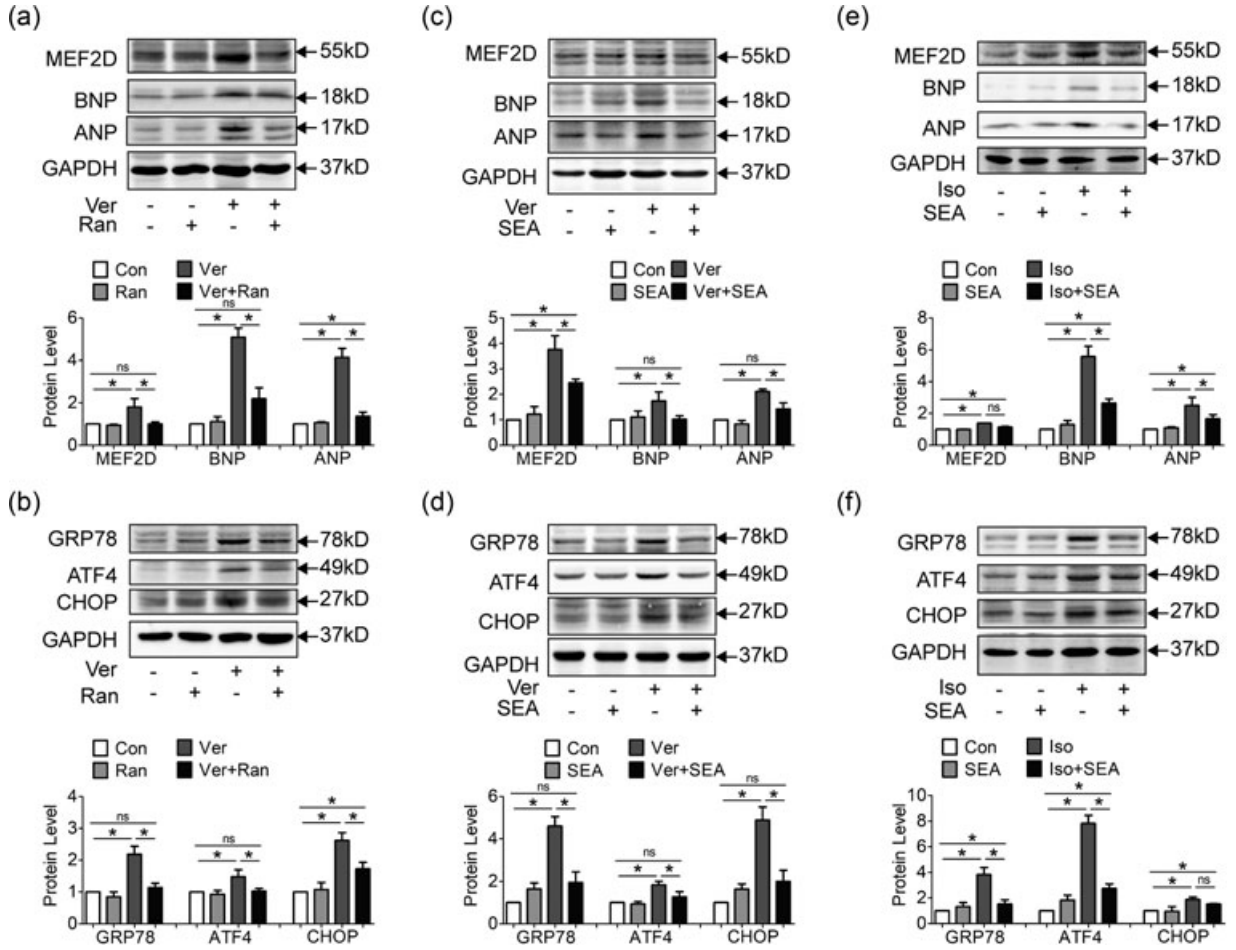

FIGURE 7 Inhibition of NCX reduces Ca^{2+}-dependent hypertrophic pathway and ER stress. (a, b) Hypertrophic markers MEF2D, ANP, and BNP (a) and ER stress markers GRP78, ATF4, and CHOP (b) were upregulated in HL-1 pretreated with Na^+ activator veratridine, while ranolazine suppressed hypertrophic pathway and ER stress induced by veratridine. (c, d) Hypertrophic markers (c) and ER stress markers (b) were upregulated in HL-1 pretreated with veratridine, while inhibition of NCX activity with SEA suppressed hypertrophic pathway and ER stress induced by veratridine. (e, f) Hypertrophic markers (e) and ER stress markers (f) were upregulated by β-agonist Isoproterenol in HL-1 cells, and inhibition of NCX activity with SEA also attenuated hypertrophy and ER stress. Each western blot analysis was performed for 3–5 biological repeats. Data were shown as mean ± standard error of the mean (*$p < 0.05$). ANP: atrial natriuretic peptide; ATF4: activating transcription factor 4; BNP: brain natriuretic peptide; CHOP: CCAAT-enhancer-binding protein homologous protein; ER: endoplasmic reticulum; GRP78: glucose-regulated protein 78; MEF2: myocyte enhancer factor-2; NCX: sodium calcium exchanger; SEA: SEA0400

overload. Based on above facts and findings in our study, we speculate that ranolazine reduces SR leak by inhibiting Na^+ induced Ca^{2+} overload, downregulating the RyR2 phosphorylation by CaMKII and reducing the P_o of RyR2. This speculation was supported by the findings in control cardiomyocytes that veratridine induced Na^+ and Ca^{2+} overload with increased SR leak and impaired SR Ca^{2+} stores, while ranolazine treatment normalized the aberrant Na^+ and Ca^{2+} handling.

Though triggered by different initial pathologic causes, cardiac hypertrophy shares some common features resulting from a genetic reprogramming of several proteins, and Ca^{2+} has been proved as a key signaling regulator in the initiation of such genetic reprogramming (Gomez, Ruiz-Hurtado, Benitah, & Dominguez-Rodriguez, 2013). As in this study, CaMKII activation is a response to elevated Ca^{2+} concentrations. Under intracellular Ca^{2+} overload, phosphorylated CaMKII increases MEF2D transcriptional activity by phosphorylating HDAC and releasing MEF2 from HDAC repression (Zhang et al., 2007). In addition, phosphorylated CaMKII activates calcineurin and promotes NFATc3 translocalize into nuclei. Both MEF2D and NFATc3 are transcription factors targeting at hypertrophic and HF gene programming. In this study, we detected the increased activity of CaMKII in TAC mice, as denoted by the phosphorylation ratio of CaMKII, which is consistent with the aberrant Ca^2 cycling in TAC mice cardiomyocytes. And Ca^{2+}/CaM/CaMKII/MEF2 and calcineurin/NFAT pathways were activated, together with overexpression of the hypertrophic and HF markers ANP and BNP. While in mice treated with ranolazine, this cascade was well inhibited. These observations were reproduced in HL-1 cell line exposed to β-agonist isoproterenol and LTCC activator Bay K8644. Together, these data suggest that ranolazine alleviated the Ca^{2+}/CaM/CaMKII/MEF2 and calcineurin/NFAT pathways by normalizing Ca^{2+} handling in cardiac hypertrophy and HF.

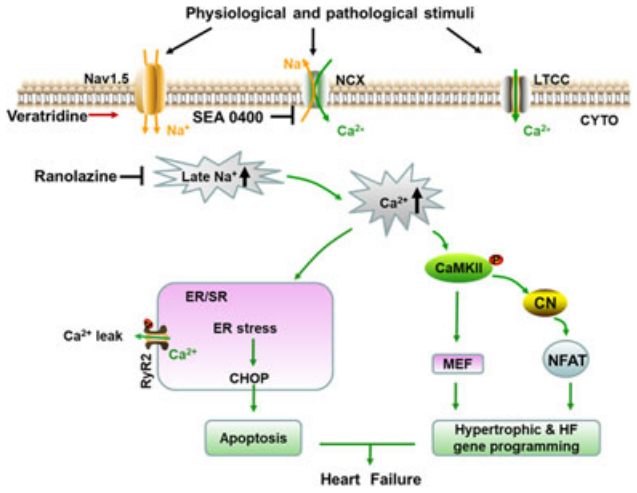

FIGURE 8 Schematic showing how ranolazine attenuates cardiac hypertrophy and heart failure. Under physiological situation, $I_{Na,L}$ constitutes a small inward sodium current, and NCX works in the forward mode to bring Na^+ in and export Ca^{2+} out of the cell membrane. While under stimuli such as pressure overload, sustained $I_{Na,L}$ makes up a considerable amount of Na^+ current, and results in an elevated concentration of intracellular Na^+, favoring the reverse mode of NCX to expel extra Na^+ and bring in more Ca^{2+}. Excessive Ca^{2+} triggers its target pathways and stress response. Under Ca^{2+} overload, Ca^{2+} leak from ER also increased, partly owing to the highly phosphorylated RyR2 by CaMKII, aggravating intracellular Ca^{2+} overload. In addition, imbalance of cytoplasmic and ER luminal Ca^{2+} handling disturb the protein folding environment and unfolded protein aggregates lead to ER stress. Prolonged ER stress upregulates the apoptotic effector CHOP to induce cell apoptosis and heart failure. Activated CaMKII releases the transcriptional activity of transcription factor MEF2D and promote nuclear translocalization of NFATc3, allowing for hypertrophic and heart failure gene programming. Together, ranolazine exerts protection by inhibition of $I_{Na,L}$ and normalizing Ca^{2+} handling, thus alleviating the downstream deterioration of cardiac structural and functional remodeling. CaM: calmodulin; CHOP: CCAAT-enhancer-binding protein homologous protein; ER: endoplasmic reticulum; MEF2: myocyte enhancer factor-2; NCX: sodium calcium exchanger; NFAT: nuclear factor of activated T-cells [Color figure can be viewed at wileyonlinelibrary.com]

The ER is the cell's protein-folding workshop. Under stress stimuli such as Ca^{2+} and ER Ca^{2+} depletion, protein folding would be suspended to reduce oxygen consumption and save energy, which results in the accumulation and aggregation of unfolded proteins—a condition referred to as ER stress (Yaoita, Sakabe, Maehara, & Maruyama, 2002). As in this study, ER chaperone GRP78 was overexpressed to deal with unfolded protein under pressure overload. Unfolded protein aggregates recruit GRP78 from ER membrane and dissociate with PERK, activating the transcription factor ATF4. ATF4 not only induces upregulation of molecular chaperones and folding enzymes, but also induces the expression of proapoptotic transcription factor CHOP (Groenendyk, Agellon, & Michalak, 2013). Pressure overload by TAC induces expression of ER chaperones and ER stress-induced apoptosis of cardiac myocytes, leading to cardiac hypertrophy and HF (Okada et al., 2004). In this study, the induction of ER stress and cell apoptosis were observed in TAC mice and ameliorated by ranolazine.

In vitro study using HL-1 cell line showed that ER stress and apoptosis were induced by both Ca^{2+} activator Bay K8644 and Na^+ activator veratridine, which opens voltage-dependent Na^+ channels and increases $[Na^+]_i$, while pretreatment of ranolazine markedly reduced ER stress signaling. Furthermore, interrupting the Na^+ induced Ca^{2+} influx by pharmacological or genetical inhibition of NCX activity attenuated ER stress and apoptosis in veratridine-treated cells, suggesting a joint role of NCX between Na^+ and Ca^{2+} crosstalk.

The effect of ranolazine in chronic HF has been investigated by many groups worldwide. And the conclusions were generally promising, revealing increased $I_{Na,L}$ in hearts of both animal models and failing human hearts, and the administration of ranolazine improved cardiac function (De Angelis et al., 2016; Flenner et al., 2016; Murray & Colombo, 2014; Sossalla & Maier, 2012; Williams, Pourrier, McAfee, Lin, & Fedida, 2014). Studies in dogs with chronic HF revealed therapeutic effect of ranolazine on left ventricular function (Rastogi et al., 2008; Undrovinas, Belardinelli, Undrovinas, & Sabbah, 2006). For clinical trials, a study of Murray's group confirmed ranolazine preserved and improved left ventricular EF and autonomic measures when added to guideline-driven therapy in 54 matched patients of chronic HF, with a mean follow-up period of 23.7 months. And the subgroup of metabolic efficiency with ranolazine for less ischemia in non-ST elevation acute coronary-thrombolysis in myocardial infarction 36 (MERLIN-TIMI 36) trial with 4,543 patients revealed that patients with elevated levels of brain natriuretic peptide (BNP > 80 pg/ml) were at higher risk of composite cardiovascular death, myocardial infarction, and recurrent ischemia at 1 year; and in these high-risk patients, ranolazine reduced the primary end point (Morrow et al., 2010).

While the current studies of ranolazine on HF came to the similar conclusions with our observations on pressure overload-induced HF, the effect of ranolazine on cardiac hypertrophy remained controversial. Among many others, Coppini Raffaele's team has done a lot of work to explore the effect of ranolazine on hypertrophic cardiomyopathy (HCM). Their research on the troponin-T mutation mouse model of HCM, cardiomyocytes and trabeculae from HCM patients (Coppini et al., 2013, 2017; Olivotto et al., 2018) all showed enhanced $I_{Na,L}$ and Ca^{2+} overload, and ranolazine improved HCM phenotype and protected cardiac function. However, Flenner et al. (2016) suggested ranolazine lacks long-term therapeutic effects in vivo in an Mybpc3-targeted knock-in mouse model of HCM. Meanwhile, the randomized, double-blind, placebo-controlled clinical trial RESTYLE-HCM, including 80 nonobstructive HCM patients aged 53 ± 14 years, revealed that ranolazine showed no overall effect on exercise performance, plasma prohormone brain natriuretic peptide levels, diastolic function, or quality of life after 5 months follow-up (Olivotto et al., 2018). What is worse, the LIBERTY-HCM Trial (NCT02291237), including 172 HCM patients aged 47 ± 11.1 years to explore the effect of another $I_{Na,L}$ inhibitor eleclazine on HCM, was terminated before the end of the double-blind phase, because the totality of the current data did not support continuation. These discrepancies were not easy to interpret.

A couple of possibilities might be put forward. (a) Onset of treatment. According to the current animal experiments (De Angelis et al., 2016; Liles et al., 2015; Rocchetti et al., 2014; Toischer et al., 2013), ranolazine was effective on cardiac hypertrophy on those acquired models, which were treated shortly after hypertrophic modeling. However, on those genetic models, hypertrophic cardiac remodeling starts since the embryonic period. Ranolazine might not be strong enough to reverse the already severe hypertrophy. A clinical trial of Ho et al. (2015) to explore the treatment of HCM also emphasized the importance of early onset of treatment. As human HCM was mainly caused by genetic mutations, this might be the major reason for the failure in HCM clinical trials. Subclinical juvenile might be the appropriate population for administration, as has performed by Ho et al. (2015). (b) Drug administration duration. According to published data, though ranolazine lacked therapeutic effects in the Mybpc3 knock-in mouse as Flenner et al (2016) reported, improvement in hypertrophic biomarkers and echocardiographic dimensions were observed. Longer duration might be essential for ranolazine to exert protection effect.

However, we still have limitations. Ranolazine is generally investigated as selective $I_{Na,L}$ inhibitor, since it exhibits higher inhibition selection than other ion currents within a certain range of concentration (Scirica et al., 2007). But its pleiotropic effect should not be ignored. Besides $I_{Na,L}$ inhibition, ranolazine also exhibits β receptor blockade, L-type Ca channel blockade as well as a block of transient outward K current. In the future, we will focus on more selective $I_{Na,L}$ inhibitor effect on cardiac hypertrophy and HF.

In summary, our study demonstrates that inhibition of $I_{Na,L}$ with ranolazine improves pressure overload-induced cardiac hypertrophy and systolic and diastolic dysfunction by normalizing Na^+ and Ca^{2+} handling, inhibiting the downstream hypertrophic pathways and ER stress. Our study provides evidence for the new clinical application of $I_{Na,L}$ inhibition.

ACKNOWLEDGMENTS

This study was supported by National Natural Science Foundation of China (Grant Nos. 81470519, 91439203, 81630010, 31771264, and 31400998) and National Institutes of Health (Grant Nos. R01-HL089598, R01-HL091947, and R01-HL117641) to X. H. T. W., and American Heart Association (Grant No. 13EIA14560061) to X. H. T. W. Murine cardiac cell line HL-1 was a kind gift from professor Claycomb. Supports from colleagues of Division of Cardiology, Department of Internal Medicine, Tongji Hospital, Tongji Medical College, Huazhong University of Science and Technology and Hubei Key Laboratory of Genetics and Molecular Mechanisms of Cardiological Disorders were acknowledged in this study.

DISCLOSURE

X. H. T. Wehrens is a founding partner of Elex Biotech, a start-up company that developed drug molecules that target ryanodine receptors for the treatment of cardiac arrhythmia disorders.

CONFLICTS OF INTEREST

The authors declare that there are no conflicts of interest.

ORCID

Zheng Wen http://orcid.org/0000-0003-4316-2459
Li Ni http://orcid.org/0000-0002-6841-4379

REFERENCES

de Almeida, P. W. M., de Freitas Lima, R., de Morais Gomes, E. R., Resende, C. R., Roman-Campos, D., Gondim, A. N. S., … Guatimosim., S. (2013). Functional cross-talk between aldosterone and angiotensin-(1-7) in ventricular myocytes. *Hypertension*, *61*, 425–430.

De Angelis, A., Cappetta, D., Piegari, E., Rinaldi, B., Ciuffreda, L. P., Esposito, G., … Berrino, L. (2016). Long-term administration of ranolazine attenuates diastolic dysfunction and adverse myocardial remodeling in a model of heart failure with preserved ejection fraction. *International Journal of Cardiology*, *217*, 69–79.

Armoundas, A. A., Hobai, I. A., Tomaselli, G. F., Winslow, R. L., & O'rourke, B. (2003). Role of sodium-calcium exchanger in modulating the action potential of ventricular myocytes from normal and failing hearts. *Circulation Research*, *93*, 46–53.

Brill, D. M., & Wasserstrom, J. A. (1986). Intracellular sodium and the positive inotropic effect of veratridine and cardiac glycoside in sheep Purkinje fibers. *Circulation Research*, *58*, 109–119.

Chaitman, B. R. (2004). Efficacy and safety of a metabolic modulator drug in chronic stable angina: Review of evidence from clinical trials. *Journal of Cardiovascular Pharmacology and Therapeutics*, *9*(Suppl 1), S47–S64.

Chelu, M. G., Sarma, S., Sood, S., Wang, S., van Oort, R. J., Skapura, D. G., … Wehrens, X. H. (2009). Calmodulin kinase II-mediated sarcoplasmic reticulum Ca^{2+} leak promotes atrial fibrillation in mice. *The Journal of Clinical Investigation*, *119*, 1940–1951.

Cingolani, O. H., Yang, X. P., Cavasin, M. A., & Carretero, O. A. (2003). Increased systolic performance with diastolic dysfunction in adult spontaneously hypertensive rats. *Hypertension*, *41*, 249–254.

Coppini, R., Ferrantini, C., Yao, L., Fan, P., Del Iungo, M., Stillitano, F., … Mugelli., A. (2013). Late sodium current inhibition reverses electromechanical dysfunction in human hypertrophic cardiomyopathy. *Circulation*, *127*, 575–584.

Coppini, R., Mazzoni, L., Ferrantini, C., Gentile, F., Pioner, J. M., Laurino, A., … Poggesi, C. (2017). Ranolazine prevents phenotype development in a mouse model of hypertrophic cardiomyopathy. *Circulation. Heart Failure*, *10*, 10.

deAlmeida, A. C., van Oort, R. J., & Wehrens, X. H. T. (2010). Transverse aortic constriction in mice. *Journal of Visualized Experiments: JoVE. J Vis Exp*, *21*(38).

Figueredo, V. M., Pressman, G. S., Romero-Corral, A., Murdock, E., Holderbach, P., & Morris, D. L. (2011). Improvement in left ventricular systolic and diastolic performance during ranolazine treatment in patients with stable angina. *Journal of Cardiovascular Pharmacology and Therapeutics*, *16*, 168–172.

Fischer, T. H., Herting, J., Mason, F. E., Hartmann, N., Watanabe, S., Nikolaev, V. O., … Sossalla, S. (2015). Late INa increases diastolic SR-Ca^{2+}-leak in atrial myocardium by activating PKA and CaMKII. *Cardiovascular Research*, *107*, 184–196.

Fischer, T. H., Herting, J., Tirilomis, T., Renner, A., Neef, S., Toischer, K., … Sossalla, S. (2013). Ca^{2+}/calmodulin-dependent protein kinase II and protein kinase A differentially regulate sarcoplasmic reticulum Ca^{2+} leak in human cardiac pathology. *Circulation*, *128*, 970–981.

Flenner, F., Friedrich, F. W., Ungeheuer, N., Christ, T., Geertz, B., Reischmann, S., … Carrier, L. (2016). Ranolazine antagonizes

catecholamine-induced dysfunction in isolated cardiomyocytes, but lacks long-term therapeutic effects in vivo in a mouse model of hypertrophic cardiomyopathy. *Cardiovascular Research*, *109*, 90–102.

Gaborit, N., Steenman, M., Lamirault, G., Le Meur, N., Le Bouter, S., Lande, G., … Demolombe, S. (2005). Human atrial ion channel and transporter subunit gene-expression remodeling associated with valvular heart disease and atrial fibrillation. *Circulation*, *112*, 471–481.

Glynn, P., Musa, H., Wu, X., Unudurthi, S. D., Little, S., Qian, L., … Hund, T. J. (2015). Voltage-gated sodium channel phosphorylation at ser571 regulates late current, arrhythmia, and cardiac function in vivo. *Circulation*, *132*, 567–577.

Gomez, A., Ruiz-Hurtado, G., Benitah, J. P., & Dominguez-Rodriguez, A. (2013). Ca(2+) fluxes involvement in gene expression during cardiac hypertrophy. *Current vascular pharmacology*, *11*, 497–506.

Groenendyk, J., Agellon, L. B., & Michalak, M. (2013). Coping with endoplasmic reticulum stress in the cardiovascular system. *Annual Review of Physiology*, *75*, 49–67.

Hayashi, T., & Su, T. P. (2007). Sigma-1 receptor chaperones at the ER-mitochondrion interface regulate Ca(2+) signaling and cell survival. *Cell*, *131*, 596–610.

Henein, M., Mörner, S., Lindmark, K., & Lindqvist, P. (2013). Impaired left ventricular systolic function reserve limits cardiac output and exercise capacity in HFpEF patients due to systemic hypertension. *International Journal of Cardiology*, *168*, 1088–1093.

Ho, C. Y., Lakdawala, N. K., Cirino, A. L., Lipshultz, S. E., Sparks, E., Abbasi, S. A., … Seidman, C. E. (2015). Diltiazem treatment for pre-clinical hypertrophic cardiomyopathy sarcomere mutation carriers: A pilot randomized trial to modify disease expression. *JACC. Heart Failure*, *3*, 180–188.

Kaye, D. M., & Krum, H. (2007). Drug discovery for heart failure: A new era or the end of the pipeline? *Nature Reviews Drug Discovery*, *6*, 127–139.

Kent, R. L., Hoober, J. K., & Cooper, G. (1989). Load responsiveness of protein synthesis in adult mammalian myocardium: Role of cardiac deformation linked to sodium influx. *Circulation Research*, *64*, 74–85.

Liles, J. T., Hoyer, K., Oliver, J., Chi, L., Dhalla, A. K., & Belardinelli, L. (2015). Ranolazine reduces remodeling of the right ventricle and provoked arrhythmias in rats with pulmonary hypertension. *The Journal of Pharmacology and Experimental Therapeutics*, *353*, 480–489.

Lou, Q., Janardhan, A., & Efimov, I. R. (2012). Remodeling of calcium handling in human heart failure. *Advances in Experimental Medicine and Biology*, *740*, 1145–1174.

Maier, L. S., & Bers, D. M. (2007). Role of Ca2+/calmodulin-dependent protein kinase (CaMK) in excitation-contraction coupling in the heart. *Cardiovascular Research*, *73*, 631–640.

Maltsev, V. A., Silverman, N., Sabbah, H. N., & Undrovinas, A. I. (2007). Chronic heart failure slows late sodium current in human and canine ventricular myocytes: Implications for repolarization variability. *European Journal of Heart Failure*, *9*, 219–227.

Mognol, G. P., Carneiro, F. R., Robbs, B. K., Faget, D. V., & Viola, J. P. (2016). Cell cycle and apoptosis regulation by NFAT transcription factors: New roles for an old player. *Cell Death & Disease*, *7*, e2199.

Morrow, D. A., Scirica, B. M., Sabatine, M. S., de Lemos, J. A., Murphy, S. A., Jarolim, P., … Braunwald, E. (2010). B-type natriuretic peptide and the effect of ranolazine in patients with non-ST-segment elevation acute coronary syndromes: Observations from the MERLIN-TIMI 36 (Metabolic Efficiency With Ranolazine for Less Ischemia in Non-ST Elevation Acute Coronary-Thrombolysis In Myocardial Infarction 36) trial. *Journal of the American College of Cardiology*, *55*, 1189–1196.

Murray, G. L., & Colombo, J. (2014). Ranolazine preserves and improves left ventricular ejection fraction and autonomic measures when added to guideline-driven therapy in chronic heart failure. *Heart International*, *9*, 66–73.

Ni, L., Zhou, C., Duan, Q., Lv, J., Fu, X., Xia, Y., & Wang, D. W. (2011). Beta-AR blockers suppresses ER stress in cardiac hypertrophy and heart failure. *PLOS One*, *6*, e27294.

Okada, K., Minamino, T., Tsukamoto, Y., Liao, Y., Tsukamoto, O., Takashima, S., … Kitakaze, M. (2004). Prolonged endoplasmic reticulum stress in hypertrophic and failing heart after aortic constriction: Possible contribution of endoplasmic reticulum stress to cardiac myocyte apoptosis. *Circulation*, *110*, 705–712.

Olivotto, I., Camici, P. G., Merlini, P. A., Rapezzi, C., Patten, M., Climent, V., … Mugelli, A. (2018). Efficacy of ranolazine in patients with symptomatic hypertrophic cardiomyopathy: The RESTYLE-HCM randomized, double-blind, placebo-controlled study. *Circulation. Heart Failure*, *11*, e004124.

Onal, B., Gratz, D., & Hund, T. J. (2017). Ca2+/calmodulin kinase II-dependent regulation of atrial myocyte late Na+ current, Ca2+ cycling and excitability: A mathematical modeling study. *American Journal of Physiology Heart and Circulatory Physiology*, *313*, 1227. ajpheart 00185 02017

Parikh, A., Mantravadi, R., Kozhevnikov, D., Roche, M. A., Ye, Y., Owen, L. J., … Salama, G. (2012). Ranolazine stabilizes cardiac ryanodine receptors: A novel mechanism for the suppression of early after-depolarization and torsades de pointes in long QT type 2. *Heart rhythm: the official journal of the Heart Rhythm Society*, *9*, 953–960.

Popescu, I., Galice, S., Mohler, P. J., & Despa, S. (2016). Elevated local [Ca2+] and CaMKII promote spontaneous Ca2+ release in ankyrin-B-deficient hearts. *Cardiovascular Research*, *111*, 287–294.

Qu, W., Zhou, Y., Zhang, Y., Lu, Y., Wang, X., Zhao, D., … Zhang, C. (2012). MFEprimer-2.0: A fast thermodynamics-based program for checking PCR primer specificity. *Nucleic acids research*. *40*, W205–208.

Rastogi, S., Sharov, V. G., Mishra, S., Gupta, R. C., Blackburn, B., Belardinelli, L., … Sabbah, H. N. (2008). Ranolazine combined with enalapril or metoprolol prevents progressive LV dysfunction and remodeling in dogs with moderate heart failure. *American Journal of Physiology Heart and Circulatory Physiology*, *295*, H2149–H2155.

Rocchetti, M., Sala, L., Rizzetto, R., Staszewsky, L. I., Alemanni, M., Zambelli, V., … Zaza, A. (2014). Ranolazine prevents INaL enhancement and blunts myocardial remodelling in a model of pulmonary hypertension. *Cardiovascular Research*, *104*, 37–48.

Scirica, B. M., Morrow, D. A., Hod, H., Murphy, S. A., Belardinelli, L., Hedgepeth, C. M., … Braunwald, E. (2007). Effect of ranolazine, an antianginal agent with novel electrophysiological properties, on the incidence of arrhythmias in patients with non ST-segment elevation acute coronary syndrome: Results from the metabolic efficiency with ranolazine for less ischemia in non ST-elevation acute coronary syndrome thrombolysis in myocardial infarction 36 (MERLIN-TIMI 36) randomized controlled trial. *Circulation*, *116*, 1647–1652.

Sossalla, S., & Maier, L. S. (2012). Role of ranolazine in angina, heart failure, arrhythmias, and diabetes. *Pharmacology & Therapeutics*, *133*, 311–323.

St-Onge, M., Dubé, P. A., Gosselin, S., Guimont, C., Godwin, J., Archambault, P. M., … Blais, R. (2014). Treatment for calcium channel blocker poisoning: A systematic review. *Clinical Toxicology*, *52*, 926–944.

Takimoto, E., Champion, H. C., Li, M., Belardi, D., Ren, S., Rodriguez, E. R., … Kass, D. A. (2005). Chronic inhibition of cyclic GMP phosphodiesterase 5A prevents and reverses cardiac hypertrophy. *Nature Medicine*, *11*, 214–222.

Toischer, K., Hartmann, N., Wagner, S., Fischer, T. H., Herting, J., Danner, B. C., … Sossalla, S. (2013). Role of late sodium current as a potential arrhythmogenic mechanism in the progression of pressure-induced heart disease. *Journal of Molecular and Cellular Cardiology*, *61*, 111–122.

Undrovinas, A. I., Belardinelli, L., Undrovinas, N. A., & Sabbah, H. N. (2006). Ranolazine improves abnormal repolarization and contraction in left ventricular myocytes of dogs with heart failure by inhibiting late sodium current. *Journal of Cardiovascular Electrophysiology*, *17*(Suppl 1), S169–S177.

Wagner, S., Dybkova, N., Rasenack, E. C. L., Jacobshagen, C., Fabritz, L., Kirchhof, P., … Maier, L. S. (2006). Ca2+/calmodulin-dependent

protein kinase II regulates cardiac Na+channels. *The Journal of Clinical Investigation*, *116*, 3127–3138.

Wehrens, X. H. T., Lehnart, S. E., Reiken, S. R., & Marks, A. R. (2004). Ca2+/calmodulin-dependent protein kinase II phosphorylation regulates the cardiac ryanodine receptor. *Circulation Research*, *94*, e61–e70.

Wehrens, X. H. T., & Marks, A. R. (2004). Novel therapeutic approaches for heart failure by normalizing calcium cycling. *Nature Reviews Drug Discovery*, *3*, 565–573.

Wilkins, B. J., & Molkentin, J. D. (2004). Calcium-calcineurin signaling in the regulation of cardiac hypertrophy. *Biochemical and Biophysical Research Communications*, *322*, 1178–1191.

Williams, S., Pourrier, M., McAfee, D., Lin, S., & Fedida, D. (2014). Ranolazine improves diastolic function in spontaneously hypertensive rats. *American Journal of Physiology Heart and Circulatory Physiology*, *306*, H867–H881.

Yaoita, H., Sakabe, A., Maehara, K., & Maruyama, Y. (2002). Different effects of carvedilol, metoprolol, and propranolol on left ventricular remodeling after coronary stenosis or after permanent coronary occlusion in rats. *Circulation*, *105*, 975–980.

Zhang, T., Kohlhaas, M., Backs, J., Mishra, S., Phillips, W., Dybkova, N., … Brown, H. (2007). CaMKIIdelta isoforms differentially affect calcium handling but similarly regulate HDAC/MEF2 transcriptional responses. *The Journal of Biological Chemistry*, *282*, 35078–35087.

SUPPORTING INFORMATION

Additional supporting information may be found online in the Supporting Information section at the end of the article.

How to cite this article: Nie J, Duan Q, He M, et al. Ranolazine prevents pressure overload-induced cardiac hypertrophy and heart failure by restoring aberrant Na^+ and Ca^{2+} handling. *J Cell Physiol*. 2018;1–15. https://doi.org/10.1002/jcp.27791